

## Inertial focusing of non-spherical microparticles

Sojung Claire Hur, Sung-Eun Choi, Sunghoon Kwon, and Dino Di Carlo

Citation: *Appl. Phys. Lett.* **99**, 044101 (2011); doi: 10.1063/1.3608115

View online: <http://dx.doi.org/10.1063/1.3608115>

View Table of Contents: <http://apl.aip.org/resource/1/APPLAB/v99/i4>

Published by the [American Institute of Physics](#).

---

### Related Articles

Vibrational frequencies of anti-diabetic drug studied by terahertz time-domain spectroscopy  
*Appl. Phys. Lett.* **100**, 143702 (2012)

On the inverse temperature transition and development of an entropic elastomeric force of the elastin mimetic peptide [LGGVG]<sub>3</sub>, 7  
*J. Chem. Phys.* **136**, 085101 (2012)

On the inverse temperature transition and development of an entropic elastomeric force of the elastin mimetic peptide [LGGVG]<sub>3</sub>, 7  
*JCP: BioChem. Phys.* **6**, 02B617 (2012)

Far-infrared spectroscopy on free-standing protein films under defined temperature and hydration control  
*JCP: BioChem. Phys.* **6**, 02B614 (2012)

Far-infrared spectroscopy on free-standing protein films under defined temperature and hydration control  
*J. Chem. Phys.* **136**, 075102 (2012)

---

### Additional information on *Appl. Phys. Lett.*

Journal Homepage: <http://apl.aip.org/>

Journal Information: [http://apl.aip.org/about/about\\_the\\_journal](http://apl.aip.org/about/about_the_journal)

Top downloads: [http://apl.aip.org/features/most\\_downloaded](http://apl.aip.org/features/most_downloaded)

Information for Authors: <http://apl.aip.org/authors>

## ADVERTISEMENT



AIP Advances

Special Topic Section:  
**PHYSICS OF CANCER**

Why cancer? Why physics? [View Articles Now](#)

## Inertial focusing of non-spherical microparticles

Soojung Claire Hur,<sup>1,2</sup> Sung-Eun Choi,<sup>3,4</sup> Sunghoon Kwon,<sup>3</sup> and Dino Di Carlo<sup>2,5,a)</sup>

<sup>1</sup>Mechanical and Aerospace Engineering Department, University of California Los Angeles, Los Angeles, California 90095, USA

<sup>2</sup>California NanoSystems Institute, Los Angeles, California 90095, USA

<sup>3</sup>Department of Electrical Engineering, Seoul National University, Seoul 151-742, South Korea

<sup>4</sup>Inter-university Semiconductor Research Center, Seoul National University Seoul, 151-742, South Korea

<sup>5</sup>Department of Bioengineering, University of California Los Angeles, Los Angeles, California 90095, USA

(Received 18 May 2011; accepted 10 June 2011; published online 29 July 2011)

We have investigated the focusing and dynamics of non-spherical polymeric particles in microfluidic flows at finite Reynolds number. The rotational diameter,  $D_{\max}$ , of a particle, regardless of its cross-sectional shape, was found to determine the final focused position, except for the case of asymmetric disks. Additionally, elongated particles with larger  $D_{\max}$  exhibited longer residence times in a horizontal orientation than those with smaller  $D_{\max}$ . These findings inform approaches to hydrodynamically control shaped and barcoded particles for multiplexed biochemical assays. © 2011 American Institute of Physics. [doi:10.1063/1.3608115]

Despite rapid advancements in the field of molecular biology, fast and information-rich identification and quantification of minute analytes remains challenging for various applications. Increase in demand for such techniques has led to development of innovative multiplexed planar and suspension biochemical assays.<sup>1,2</sup> Particularly, suspension assays utilizing multifunctional encoded microparticles as an active analyte-binding substrate<sup>3,4</sup> were reported to be more advantageous than current time- and labor-intensive planar assays (e.g., microarray and Enzyme-Linked Immunosorbent Assay (ELISA)), owing to their higher sample throughput and probe-set flexibility. Unlike spectral encoding, spatial barcoding techniques eliminate the need for a complex optical detection setup and enable an almost limitless number of encoding combinations. Recently, barcoded microparticles, synthesized using stop flow lithography, were used to demonstrate multiplexed biochemical assays with high-throughput.<sup>3,5,6</sup> However, despite success in automated detection and manipulation of such particles, the requirements of sheath flow and active guiding techniques<sup>7,8</sup> limit the further improvement of throughput desired for clinical applications. Hence, a method of particle manipulation in a high-throughput manner without sheath-flow or active guiding is needed.

Inertial focusing allows manipulation and separation of microparticles/cells in such a manner utilizing only intrinsic hydrodynamic forces.<sup>9</sup> An increase in overall processing speed can be attained with inertial focusing due to its intrinsically high operational flow rate combined with its sheath-less focusing ability, allowing massive parallelization.<sup>10</sup> For particle-based assays, the orientation, the position, and the rotational behavior of focused flowing particles are all important parameters to determine. Particularly, the effect of inertial lift forces on nonspherical particles is important to understand for future high throughput barcode detection applications, since they would inevitably require

high operational flow rates. Thus far, however, only spherical or discoid shapes have been examined in inertial flows.

In addition to the barcoding application, inertial focusing of nonspherical particles will be of interest to other research areas. There are many arbitrarily shaped particles widely studied in biology and industrial processing<sup>11</sup> that would be important to either separate or focus for counting purposes. Therefore, how particle shape affects focusing position in a channel is important to investigate.

In this study, we investigate inertial effects on nonspherical particles with various size, cross-sectional shape, and asymmetry using single-layered straight rectangular microchannels over a wide flow rate range. Various anisotropic particles were synthesized by an optofluidic maskless lithography setup<sup>12</sup> combined with the stop-flow lithography technique<sup>13</sup> (Figures 1(b)–1(d)). Spheres and doublets were synthesized by emulsifying polydimethylsiloxane in deionized water with surfactant, followed by thermal curing.<sup>14</sup> Detailed experimental procedures can be found in supplementary material.<sup>15</sup>

Inertial focusing of the created microparticles was assessed by injecting particle suspensions through a

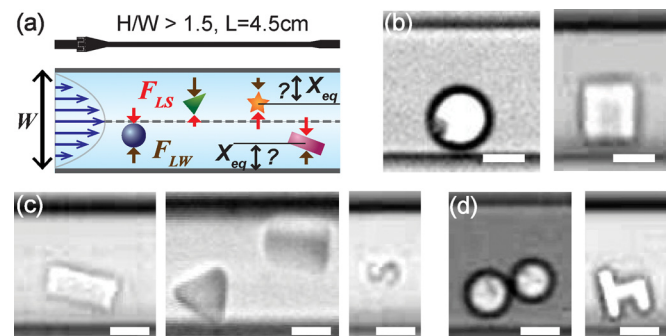


FIG. 1. (Color online) (a) Device design and schematic showing inertial forces, namely, the wall effect,  $F_{LW}$ , and the shear-gradient lift,  $F_{LS}$ , acting on microparticles, resulting in different average lateral equilibrium positions,  $X_{eq}$ . High-speed microscopic images of (b) spheres and symmetric disks, (c) cylinders with various cross-sections and aspect ratios, and (d) an asymmetric doublet and h-shaped disk.

<sup>a)</sup> Author to whom correspondence should be addressed. Electronic mail: dicarlo@seas.ucla.edu.

microchannel at an overall flow rate,  $Q$ , ranging from 25 to 1400  $\mu\text{l}/\text{min}$ . Our initial studies with cylindrical particles suggested that the behavior of flowing non-spherical particles could be very complex and drastically varied with the channel Reynolds number,  $R_c = \frac{\rho U_m D_h}{\mu}$ . Here,  $\rho$ ,  $U_m$ , and  $\mu$  are the density, the maximum velocity, and the kinematic viscosity of the fluid, respectively, whereas  $D_h$  is the hydraulic diameter of the channel, defined as  $D_h = \frac{2WH}{W+H}$ , where  $W$  and  $H$  is the channel width and height, respectively. Multiple particles flowing with a periodically consistent motion were grouped together and categorized as “focused,” “bouncing,” and “translating,” respectively, while the remaining individual particles without a motion in common were classified as “Other.” The “translating” mode (i.e., particles flowing at the channel centerline without a tumbling motion) was found to be very unstable since the behavior was observed for only a few particles flowing at low flow rate ( $R_c = 14$ ), and quickly dissipated downstream with increasing fluid inertia. At moderate flow rates ( $14 < R_c < 28$ ), the majority of cylindrical particles (>81%) exhibited a “bouncing” motion<sup>15</sup> (i.e., particles periodically translated back and forth across the channel centerline, see Figure 2(a)). The cause of this periodic cross-streamline migration, however, is still unclear and further investigation would be important to identify what leads to a transition from bouncing to focusing and rotating. As the fluid

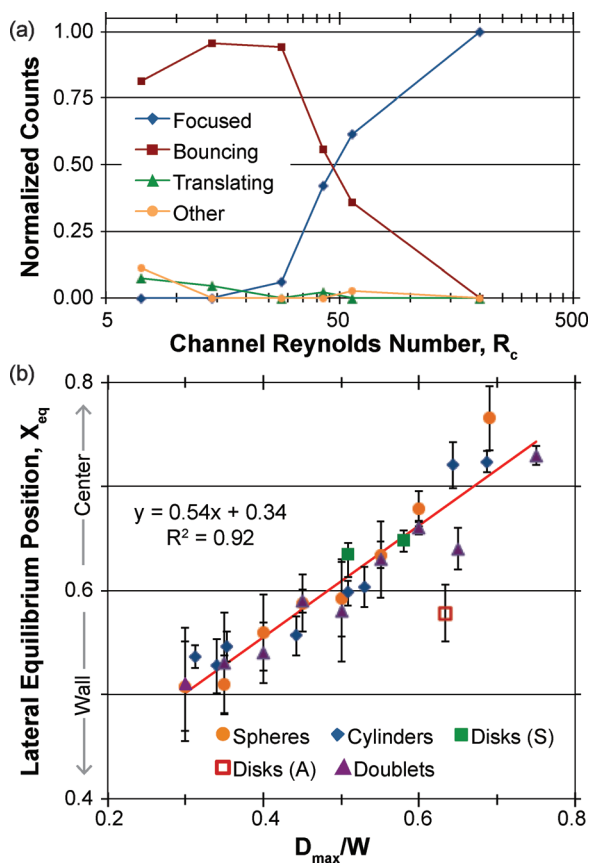


FIG. 2. (Color online) Flow rate and rotational diameter affect inertial focusing. (a) Behavior of flowing cylindrical particles at 4.5 cm downstream varied as flow rate increased. (b) Microparticles with various shapes can be inertially focused at uniform lateral and vertical locations at  $R_c = 200$ . Regardless of cross-sectional shape or aspect ratio, all particles followed the focusing trend of spheres with similar  $D_{max}$  except for asymmetric disks with an h-shaped cross-section.

inertia increases ( $R_c > 43$ ), however, particles begin to inertially focus at two streamlines (i.e., “focused” mode) and, finally, at  $R_c = 200$ , all particles were inertially focused and rotating at two lateral distinct locations near the channel walls and at the middle vertical plane<sup>15</sup>, similar to that observed for spheres in rectangular channels.<sup>10</sup> Thus, further empirical investigations on inertial focusing of nonspherical particles were conducted only at  $R_c = 200$ .

The experimental results conducted at  $R_c = 200$  revealed distinct rotational orientations for disks and cylinders, which agreed well with previous computational analysis.<sup>16</sup> As discussed in the previous study, the vorticity direction (the z-axis for the current study) was the stable orbital axis, and regardless of their aspect ratios (ARs) or cross-sectional shapes, cylinders and disks exhibited “tumbling” and “log-rolling” motion, respectively.<sup>15</sup> Importantly, for possible separations based on particle shape, the rotational diameter,  $D_{max}$ , was found to be the important dimension for nonspherical particles that determines the lateral equilibrium position,  $X_{eq}$ , among many other dimensionless parameters.<sup>15</sup> All tested particles, except disks with an “h-shaped” cross-section (referred to as h-particles hereafter), followed the similar focusing trend of spheres when  $X_{eq}$  was plotted versus  $D_{max}$  (Figure 2(b)). The h-particle was identified as an outlier since both the coefficient of determination for the linear regression,  $R^2$ , and Cook’s distance,<sup>17</sup>  $C_i$ , predicted it as the most influential data point.<sup>15</sup>

In order to investigate whether this dissimilar behavior of h-particles originated from its reduction in symmetry, we evaluated  $X_{eq}$  for doublets with various rotational diameters,

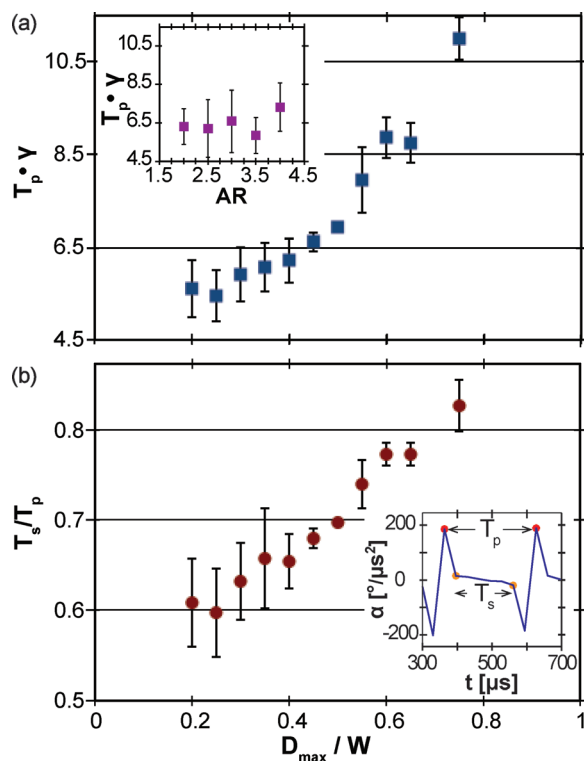


FIG. 3. (Color online) Rotational behavior of doublets with various size and asymmetry. (a) Nondimensionalized rotational period of doublets,  $T_p \cdot \gamma$ , and (b) the period ratio,  $T_s/T_p$ , were strongly dependent on  $D_{max}$  and independent of AR (inset (a)). Inset (b): definition of  $T_s/T_p$ . Here,  $\alpha$  is the magnitude of the angular acceleration of the doublet.

$D_{\max} = D_1 + D_2$ ,  $AR = D_{\max}/D_1$ , and diameter ratios,  $DR = D_1/D_2$ . Here,  $D_1$  and  $D_2$  are diameters of spheres comprising the doublet and  $D_2 \leq D_1$ . Slight fluctuations in the doublet center of mass,  $CM_D$ , were observed as doublets rotate,<sup>15</sup> and the magnitude of deviation in lateral equilibrium positions,  $\Delta X_{\text{eq}}$ , was found to increase with  $D_{\max}$ . Thus, an average value of  $CM_D$  was taken to be  $X_{\text{eq}}$  for a doublet with a given  $D_{\max}$ . Still, for these particles a similar trend for  $X_{\text{eq}}$  as that of spheres with similar diameters was observed (Figure 2(b)).

In contrast to  $D_{\max}$ , a clear correlation between  $X_{\text{eq}}$  of doublets and AR and DR was not found<sup>15</sup> (Figure 3(a)), suggesting that the asymmetry in shapes would not significantly contribute to the variation in  $X_{\text{eq}}$ . Hence, one can creatively design various particles with large surface area promoting chemical reactions or with easily distinguishable shapes, but still accurately predict their  $X_{\text{eq}}$  as long as  $D_{\max}$  is controlled carefully. The ability to synthesize particles with shapes having distinctive and predictable  $X_{\text{eq}}$  can also lead to accurate and passive purification of such particles based on  $X_{\text{eq}}$  differences.<sup>14,18,19</sup>

The origin of dissimilar behavior between the asymmetric disk (h-particle) and cylinder (doublets) is still not clear. Presumably, however, it can be attributed to (i) even greater asymmetry of h-particles compared to asymmetric doublets, (ii) different lift forces that rod-like and plate-like particles would experience, and/or (iii) additional complex flows in asymmetric void areas of an h-particle's cross-section, introducing additional lift force. Further study would be required to clarify this discrepancy.

Finally, rotational behavior of anisotropic particles in shear flow was investigated using doublets. Doublets resided longer at the horizontal orientation and least at the vertical orientation during the course of rotation. This behavior greatly resembles the classic Jeffrey orbits.<sup>20</sup> Figure 3(a) shows that the nondimensionalized rotational period,  $T_p \cdot \gamma$ , increased with  $D_{\max}$ , but was independent of AR (inset). Here,  $\gamma = \frac{u_m}{W/2}$  is an average shear rate of the channel flow. This trend agreed well with the previous numerical analysis, reporting an increase in Jeffrey orbit period with increasing length of rod-like fibers in shear flow.<sup>21</sup> Moreover, the ratio between the time that the doublet spent at horizontal orientations,  $T_h$ , and  $T_p$  was found to be proportional to  $D_{\max}$ , suggesting that the cylinders with larger  $D_{\max}$  would reside longer at a horizontal orientation and recover that orientation more rapidly than the smaller particles. This longer residence time and rapid recovery of preferred orientation would particularly benefit applications, requiring accurate orientation control for encoded shape- or pattern-recognition. Furthermore, the sheathless particle manipulating ability should have great potential to enable high-throughput multiplexed particle-based bioassays by integrating a massively parallel focusing system<sup>10</sup> with a wide-field of view optical detection technique.<sup>22</sup>

In conclusion, we have found that inertial effects can be utilized to focus nonspherical microparticles at uniform lateral and vertical locations. For most cases, the cross-sectional shape does not significantly contribute to differences in  $X_{\text{eq}}$ . Instead, among many other particle dimensions, we found that  $D_{\max}$  determines  $X_{\text{eq}}$  and can be used to predict the behavior of the flowing particles. Thus, particles with various shapes (e.g., shapes that have large surface areas allowing rapid chemical reaction) can be designed, passively focused, and used for high-throughput multiplex bioassays. Furthermore, it is found that elongated particles preferred the horizontal orientation as they rotate, suggesting that the particles with larger  $D_{\max}$  would be more useful for applications requiring accurate orientation control for reading of patterns on the particle surface.

The authors thank Henry Tse, Mahdokht Masaeli, Wook Park, and Richard Yau for their help. This work is partially supported by National Science Foundation (Grant No. 0930501) and by the Korea Science and Engineering Foundation (Grant No. 2010-0017860) funded by the Korea government (MEST).

- <sup>1</sup>L. Fabris, M. Schierhorn, M. Moskovits, and G. C. Bazan, *Small* **6**(14), 1550 (2010).
- <sup>2</sup>J. Hong, J. B. Edel, and A. J. deMello, *Drug Discovery Today* **14**(3–4), 134 (2009).
- <sup>3</sup>H. Lee, J. Kim, H. Kim, and S. Kwon, *Nat. Mater.* **9**(9), 745 (2010).
- <sup>4</sup>D. C. Pregibon, M. Toner, and P. S. Doyle, *Science* **315**(5817), 1393 (2007).
- <sup>5</sup>S. C. Chapin, D. C. Appleyard, D. C. Pregibon, and P. S. Doyle, *Angew. Chem.* **123**(10), 2337 (2011).
- <sup>6</sup>D. C. Appleyard, S. C. Chapin, and P. S. Doyle, *Anal. Chem.* **88**(1), 193 (2010).
- <sup>7</sup>S. E. Chung, W. Park, S. Shin, S. A. Lee, and S. Kwon, *Nat. Mater.* **7**(7), 581 (2008).
- <sup>8</sup>S. H. Lee, S.-E. Choi, A. J. Heinz, W. Park, S. Han, Y. Jung, and S. Kwon, *Small* **6**(23), 2668 (2010).
- <sup>9</sup>D. Di Carlo, *Lab Chip* **9**, 3038 (2009).
- <sup>10</sup>S. C. Hur, H. T. K. Tse, and D. Di Carlo, *Lab Chip* **10**(3), 274 (2010).
- <sup>11</sup>C. R. Amenábar, M. Di Pasquo, H. Carrizo, and C. L. Azcuy, *Ameghiniana* **43**(2), 339 (2006).
- <sup>12</sup>T. Chung and H. Kim, *Electrophoresis* **28**(24), 4511 (2007).
- <sup>13</sup>D. Dendukuri, S. S. Gu, D. C. Pregibon, T. A. Hatton, and P. S. Doyle, *Lab Chip* **7**(7), 818 (2007).
- <sup>14</sup>S. C. Hur, N. K. Henderson-MacLennan, E. R. B. McCabe, and D. Di Carlo, *Lab Chip* **11**, 912 (2011).
- <sup>15</sup>See supplementary material at <http://dx.doi.org/10.1063/1.3608115> for detailed experimental and analytical methods used to understand behavior of non-spherical particles flowing in microchannels based on particle size and shape and fluidic inertia.
- <sup>16</sup>D. Qi and L. Luo, *Phys. Fluids* **14**, 4440 (2002).
- <sup>17</sup>K. A. Bollen and R. W. Jackman, *Modern Methods of Data Analysis* (Sage Publication, Newbery Park, CA, 1990), p. 257.
- <sup>18</sup>D. Di Carlo, J. F. Edd, D. Irimia, R. G. Tompkins, and M. Toner, *Anal. Chem.* **80**(6), 2204 (2008).
- <sup>19</sup>A. J. Mach and D. Di Carlo, *Biotechnol. Bioeng.* **107**(2), 302 (2010).
- <sup>20</sup>G. B. Jeffery, *Proc. R. Soc. London. Ser. A* **102**(715), 161 (1922).
- <sup>21</sup>C. G. Joung, *Rheol. Acta* **46**(1), 143 (2006).
- <sup>22</sup>T. Su, S. Seo, A. Erlinger, and A. Ozcan, *Biotechnol. Bioeng.* **102**(3), 856 (2009).